Selective activation of FGFR4 by an FGF19 variant does not improve glucose metabolism in *ob/ob* mice

Xinle Wu[a,1], Hongfei Ge[a], Bryan Lemon[a], Jennifer Weiszmann[a], Jamila Gupte[a], Nessa Hawkins[b], Xiaofan Li[a], Jie Tang[a], Richard Lindberg[a], and Yang Li[a,1]

[a]Amgen Inc., 1120 Veterans Boulevard, South San Francisco, CA 94080; and [b]Amgen Inc., One Amgen Center Drive, Thousand Oaks, CA 91320

FGF19 is a hormone that regulates bile acid and glucose homeostasis. Progress has been made in identifying cofactors for receptor activation. However, several functions of FGF19 have not yet been fully defined, including the actions of FGF19 on target tissues, its FGF receptor specificity, and the contributions of other cofactors, such as heparin. Here, we explore the requirements for FGF19-FGFR/co-receptor interactions and signaling in detail. We show that βKlotho was essential for FGF19 interaction with FGFRs 1c, 2c, and 3c, but FGF19 was able to interact directly with FGFR4 in the absence of βKlotho in a heparin-dependent manner. Further, FGF19 activated FGFR4 signaling in the presence or absence of βKlotho, but activation of FGFRs 1c, 2c, or 3c was completely βKlotho dependent. We then generated an FGF19 molecule, FGF19dCTD, which has a deletion of the C-terminal region responsible for βKlotho interaction. We determined that βKlotho-dependent FGFR1c, 2c, and 3c interactions and activation were abolished, and βKlotho-independent FGFR4 activation was preserved; therefore, FGF19dCTD is an FGFR4-specific activator. This unique FGF19 molecule specifically activated FGFR4-dependent signaling in liver and suppressed CYP7A1 expression in vivo, but was unable to activate signaling in adipose where FGFR4 expression is very low. Interestingly, unlike FGF19, treatment of *ob/ob* mice with FGF19dCTD failed to improve glucose levels and insulin sensitivity. These results suggest that FGF19-regulated liver bile acid metabolism could be independent of its glucose-lowering effect, and direct FGFR activation in adipose tissue may play an important role in the regulation of glucose homeostasis.

diabetes | liver | FGF21

The FGF19 subfamily of fibroblast growth factors (FGFs), consisting of FGF19, FGF21, and FGF23, has been implicated in the regulation of many metabolic processes (1–4). One of the properties of this subfamily is atypical heparin binding (5). FGFs generally have a positively charged heparin-binding region that helps create high-affinity interactions with cell surface FGF receptors (FGFRs) (6). Compared with other FGFs, the crystal structures of FGF19 and FGF23 revealed a disrupted heparin-binding motif, which could weaken interactions with heparin or heparan sulfate (5, 7). Consistent with this, direct measurement of affinity for immobilized heparin showed that FGF21 did not interact with heparin and that FGF19 and FGF23 bound to heparin weakly compared with the affinity of immobilized heparin for the other FGFs (6). Consequently, members of this subfamily may not be retained by heparin-containing tissues or the extracellular matrix, thus making it possible for them to function as endocrine hormones.

Another distinctive feature of this subfamily is the requirement for the co-receptors αKlotho or βKlotho in FGFR signaling complexes (8–11). With reduced affinity toward heparin, FGF19, 21, and 23 may use αKlotho or βKlotho proteins to stabilize their interactions with FGFRs to activate downstream signaling pathways. This requirement for either αKlotho or βKlotho provides another level of selectivity to FGFR signaling and may restrict the target tissues for this endocrine FGF subfamily. We showed that the Klotho-interaction domain of FGF19 subfamily members resides in their C-terminal region

(12). The sole exception for this co-receptor requirement is the ability of FGF19 to bind directly to FGFR4, but not to other FGFRs, in the absence of the Klothos (11, 13). Binding of FGF19 to FGFRs 1c, 2c, and 3c has been reported to require βKlotho (14). However, the potential differences in co-receptor requirements with different FGFRs remain to be fully defined. The ability of FGF19 to signal in certain contexts in the absence of Klotho has not been previously reported.

FGF19 regulates bile acid homeostasis and is thought to be the hormone that transmits the enterohepatic regulatory signals for bile acid synthesis (1). Administration of recombinant mouse FGF15 or FGF19 to mice decreased the expression of cholesterol 7-alpha-hydroxylase (CYP7A1), the first and rate-limiting enzyme in the classical bile acid biosynthetic pathway in the liver (1, 15). This effect is believed to be mediated through activation of FGFR4, the predominant FGFR expressed in mature hepatocytes, because FGF15-induced CYP7A1 repression was lost in *fgfr4*$^{-/-}$ mice (1, 15).

Effects of FGF19 on glucose and energy homeostasis has also been reported (2). When challenged with a high fat diet, transgenic mice over-expressing FGF19 have lower serum glucose levels, improved glucose tolerance, and improved insulin sensitivity, compared with their wild-type littermates (2, 16). Similar observations were made upon treatment of *ob/ob* mice with recombinant human FGF19. The treated mice exhibited lower serum glucose levels and improved insulin sensitivity (2, 16). These results suggest that in addition to the ability to regulate bile acid metabolism, FGF19 also exerts effects on glucose and energy metabolism. However, the underlying mechanism and the target tissues for such effects are not fully understood.

In the present study, we explored the heparin and βKlotho requirements for FGF19 signaling in detail using binding and signaling assays. In addition, we generated an FGF19 molecule in which the C-terminal region responsible for βKlotho interaction was completely removed. This novel FGF19 protein selectively activated FGFR4 signaling in liver and has proven to be a valuable tool for understanding which FGFRs and which tissues are involved in FGF19 actions.

Results

Co-Factor Requirements for FGF19/FGFR4 Are Distinct from FGF19/FGFR1–3c. To study the receptor specificity for FGF19, we used rat myoblast L6 cells, which express little endogenous FGFRs, and do not respond to FGF treatment. These cells were transfected with FGFR1c, 2c, 3c, or 4 either in the presence (Fig. 1*A*)
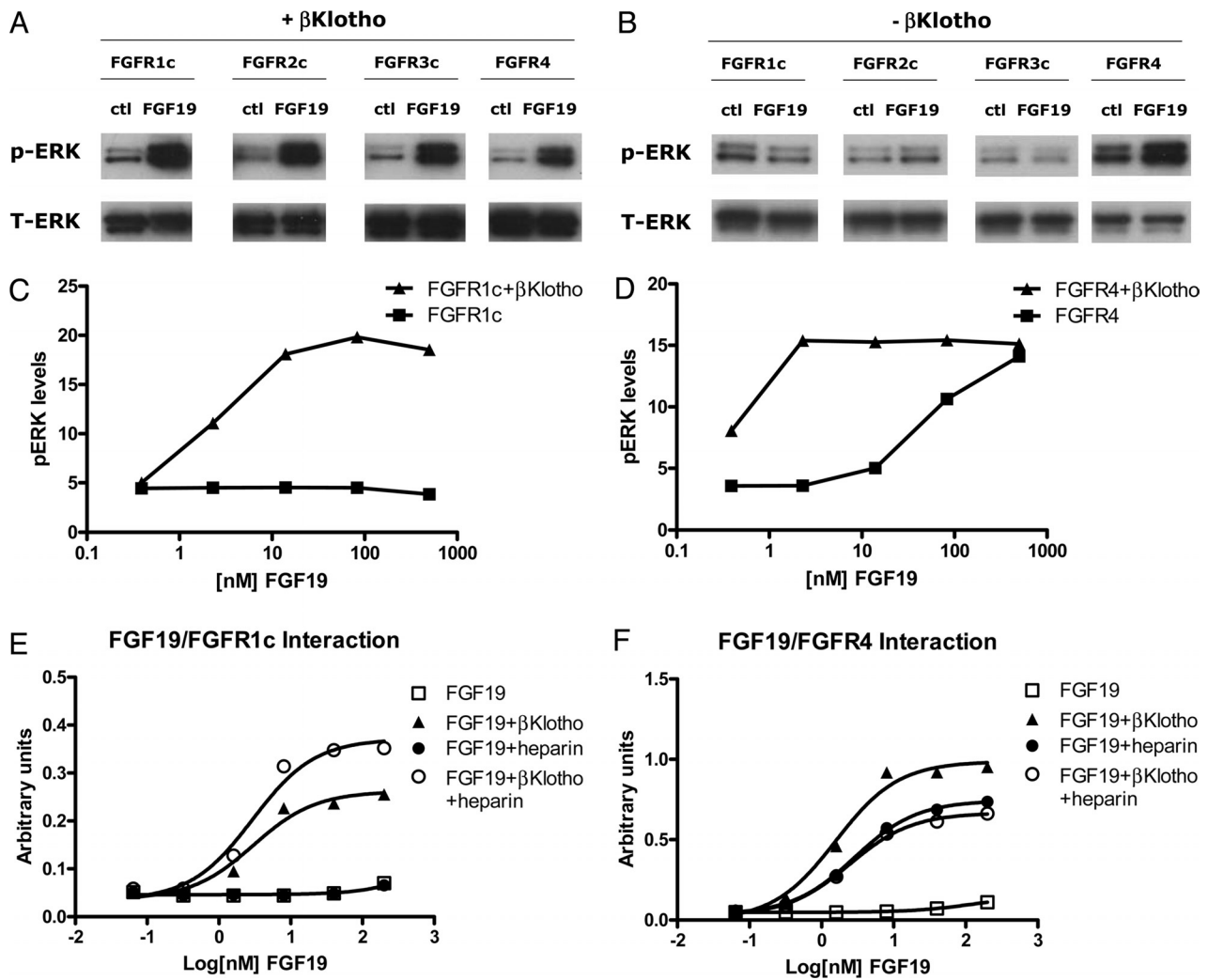
CELL BIOLOGY

Fig. 1. In vitro activity of FGF19. (*A*) L6 cells were co-transfected with expression vectors for FGFR1c, 2c, 3c, or 4 and βKlotho. Following overnight serum starvation, cells were stimulated with vehicle or 50 nM recombinant FGF19 for 15 min and snap frozen in liquid nitrogen. Cell lysates were prepared for Western blot analysis using antibodies against phosphorylated ERK1/2 (pERK) or total ERK1/2 (T-ERK). (*B*) Similar assay as (*A*) in the absence of βKlotho co-transfection. (*C*) L6 cells were transfected with FGFR1c with or without βKlotho. Following overnight serum starvation, cells were stimulated with recombinant FGF19 for 15 min and snap frozen in liquid nitrogen. Cell lysates were prepared for an MSD assay measuring phosphorylated ERK1/2 level. (*D*) Similar to (*C*), L6 cells transfected with expression vectors for FGFR4 with or without βKlotho and treated with FGF19. (*E*) Solid-phase binding assay measuring the interaction between FGFR1c and FGF19 in the presence of heparin or βKlotho. (*F*) Solid-phase binding assay measuring the interaction between FGFR4 and FGF19. "ctl" indicates no FGF control, "pERK" indicates phosphorylated ERK, "T-ERK" indicates total ERK.

or absence (Fig. 1*B*) of βKlotho. Signaling in response to FGF19 treatment was then assessed by measuring phospho-ERK (pERK) levels by Western blot analysis. Co-transfection of βKlotho enabled L6 cells to respond to FGF19 treatment with the activation of all four FGFRs: 1c, 2c, 3c, and 4 (Fig. 1*A*). However, in the absence of βKlotho, FGF19 was only able to induce ERK phosphorylation in cells transfected with FGFR4 (Fig. 1*B*). FGFR1c and FGFR4 were then chosen as representative receptors for subsequent characterization. To provide a more quantitative measurement of receptor activation, we used the MSD assay to measure pERK levels in treated L6 cells. Similar to the results of Western blotting analysis, no pERK signal was observed with FGF19-treated L6 cells transfected with FGFR1c alone, as βKlotho was required for signaling through FGFR1c (Fig. 1*C*). In contrast, transfection of FGFR4 alone was sufficient to enable L6 cells to respond to FGF19 treatment; however, co-transfection of βKlotho increased FGF19 potency (Fig. 1*D*). To ensure that the observed differential effects on FGFR1c and FGFR4 were not artifacts of the

assay, we also measured receptor autophosphorylation and FRS2 phosphorylation (a downstream substrate of FGFR); the results are consistent with ERK phosphorylation and further supported our conclusion (Fig. S1).

To further understand the contributions of co-factors to FGF19/FGFR interactions, we developed a solid-phase assay to directly measure interactions between FGF19, FGFRs, βKlotho, and heparin (Fig. 1 *E* and *F*). In the absence of both heparin and βKlotho, no direct interaction could be observed between FGF19 and FGFR1c or FGFR4. When βKlotho was present, FGF19 was able to interact with both FGFR1c and FGFR4. However, the major difference between the ability of FGF19 to interact with FGFR1c and FGFR4 was found to be the contribution of heparin. In the absence of βKlotho, FGF19 was able to interact with FGFR4 but not FGFR1c in the presence of heparin, albeit at a concentration of 10 μg/mL (compare Fig. 1 *E* and *F*). This suggests that FGF19-induced FGFR4 activation in the absence of βKlotho in L6 cells (Fig. 1 *B* and *D* and Fig. S1) may be induced by the heparan sulfate present on the cell surface. Given the observed lack of heparin-
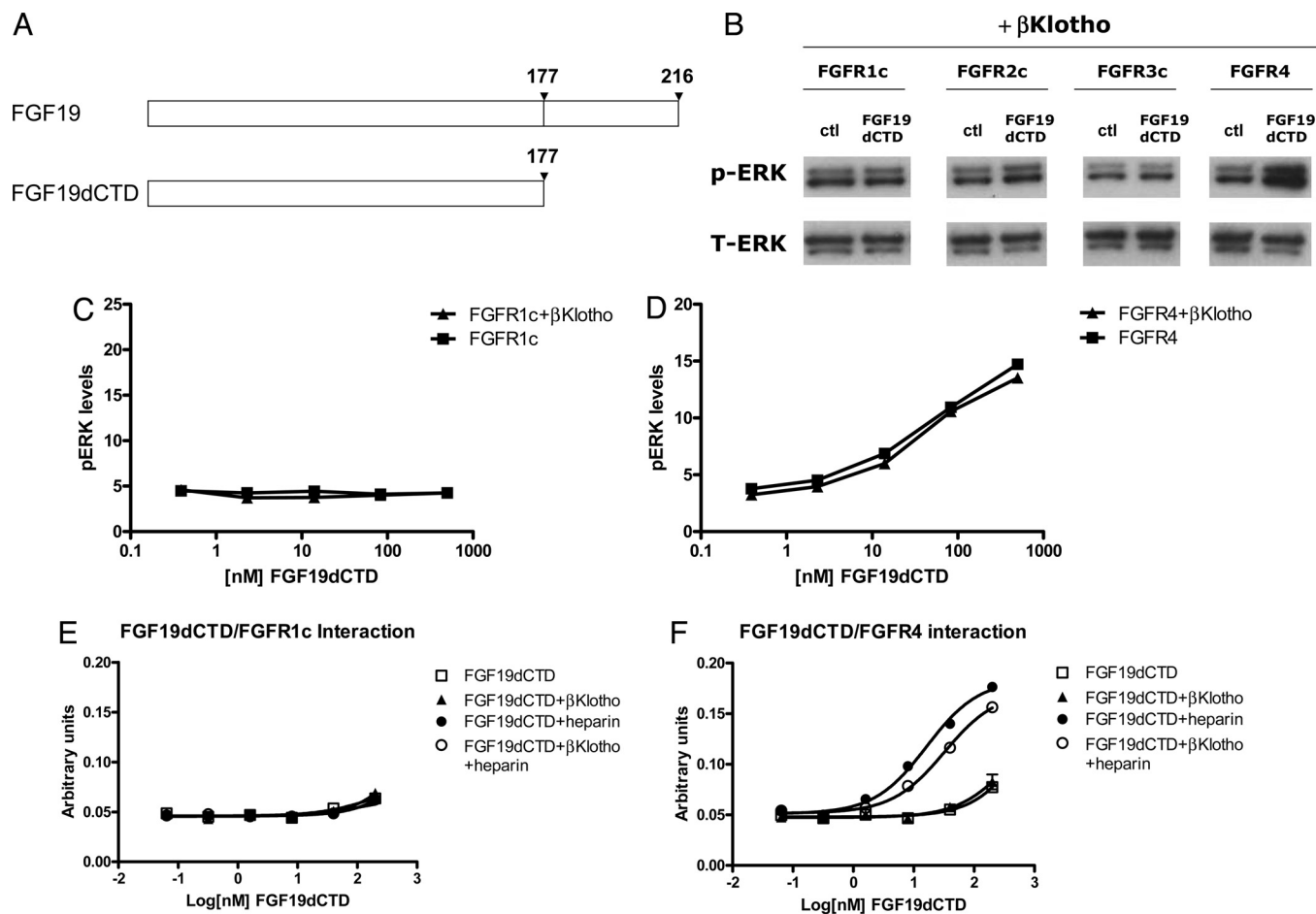
Fig. 2. In vitro activity of FGF19dCTD. (*A*) Schematic diagram showing FGF19 and FGF19dCTD. (*B*) L6 cells were transfected with expression vectors for FGFR1c, 2c, 3c, and 4 as well as βKlotho. Following overnight serum starvation, cells were stimulated with vehicle or 50 nM recombinant FGF19 for 15 min and snap frozen in liquid nitrogen. Cell lysates were prepared for Western blot analysis using antibodies against phosphorylated ERK1/2 (pERK) or total ERK1/2 (T-ERK). (*C*) L6 cells were transfected with FGFR1c with or without βKlotho. Following overnight serum starvation, cells were stimulated with recombinant FGF19dCTD for 15 min and snap frozen in liquid nitrogen. Cell lysates were prepared for an MSD assay measuring phosphorylated ERK1/2 level. (*D*) Similar to (*C*), L6 cells were transfected with expression vectors for FGFR4 with or without βKlotho and treated with FGF19dCTD. (*E*) Solid-phase binding assay measuring the interaction between FGFR1c and FGF19dCTD in the presence of heparin or βKlotho. (*F*) Solid-phase binding assay measuring the interaction between FGFR4 and FGF19dCTD.

induced interaction between FGF19 and FGFR1c, the activation of receptors other than FGFR4 may be completely dependent on βKlotho.

Generation of an FGF19 Molecule Able To Selectively Activate FGFR4. To provide further evidence for differential co-factor requirements between FGF19 and FGFR1c or FGFR4, and to understand the physiological effects of selective FGFR4 activation, we sought to generate an FGF19 molecule that could separate heparin- and βKlotho-dependent effects. We showed previously that the C-terminal domain of FGF19 subfamily members interacts with and determines Klotho specificity, and that the N-terminal region of FGF19 is responsible for heparin-dependent interactions (12). Therefore, we reasoned that if the primary function of the C-terminal domain is to enable FGF19 to interact with βKlotho, then deletion of this domain should eliminate the biological activities of FGF19 that depend on βKlotho. Such a molecule, FGF19dCTD, was generated whereby the C-terminal domain of FGF19 was completely removed (Fig. 2*A*). Consistent with our hypothesis, FGF19dCTD was unable to elicit ERK phosphorylation in L6 cells co-transfected with βKlotho and FGFR1c, 2c or 3c, but FGFR4 activation was retained (Fig. 2*B*). This was further confirmed in MSD assays, where a lack of p-ERK signaling in the presence or

absence of βKlotho on FGFR1c was observed with FGF19dCTD (Fig. 2*C*). Interestingly, in contrast to the wild-type FGF19 protein, co-transfection of βKlotho and FGFR4 did not change the dose–response curve of FGF19dCTD (compare Fig. 1 *D* with Fig. 2*D*), suggesting that the βKlotho-dependent effects were indeed abolished.

To ensure the induction of ERK phosphorylation by FGF19 and FGF19dCTD were mediated by FGFR activation, FGFR autophosphorylation and FRS2 phosphorylation were also measured (Fig. S1), and the results were consistent with ERK phosphorylation data. In addition, to rule out the possibility that the activation of L6 cells transfected with FGFR4 alone was caused by up-regulation of endogenous βKlotho, we measured the expression level of βKlotho in L6 cells with or without FGFR4 transfection and found no up-regulation of βKlotho by FGFR4 transfection. In both cases, the expression levels of endogenous βKlotho in L6 cells were very low compared with a positive control cell line, H4IIE cells (Fig. S2).

Consistent with the signaling assays, FGF19dCTD failed to interact with FGFR1c in the presence of either heparin or βKlotho in vitro (Fig. 2*E*). FGF19dCTD required heparin to bind to FGFR4 (Fig. 2*F*), and its interaction with heparin did not appear to be significantly affected by the C-terminal deletion, as a similar heparin dose curve for FGFR4 binding was observed
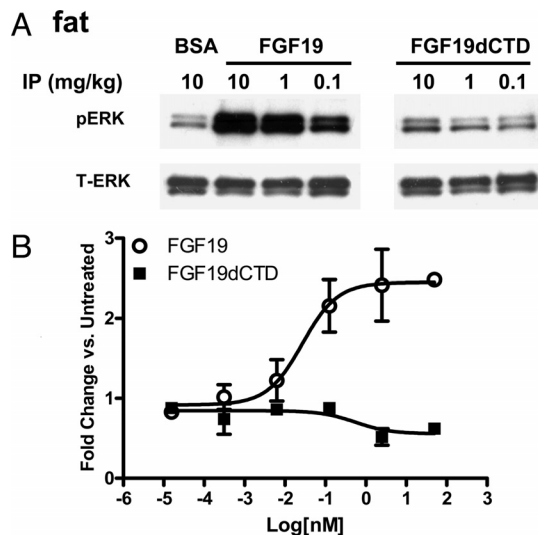
CELL BIOLOGY

Fig. 3. FGF19 and FGF19dCTD signaling in adipose tissue. (*A*) Adipose tissue was excised from *ob/ob* mice (four animals per group) treated with 10 mg/kg BSA (BSA), FGF19, or FGF19dCTD (at 0.1, 1, or 10 mg/kg) 15 min after injection. Tissue lysates were prepared and pooled for Western blot analysis using phosphorylated ERK1/2 (pERK) or total ERK1/2 (T-ERK) antibodies. (*B*) Differentiated 3T3-L1 adipocytes were incubated for 72 h with recombinant FGF19 or FGF19dCTD and assayed for glucose uptake.

Fig. 4. FGF19 and FGF19dCTD signaling in liver. (*A*) Livers were excised from *ob/ob* mice (four animals per group) treated with 10 mg/kg BSA (BSA), FGF19, or FGF19dCTD (at 0.1, 1, or 10 mg/kg) 15 min after injection. Tissue lysates were prepared and pooled for Western blot analysis using phosphorylated ERK1/2 (pERK) or total ERK1/2 (T-ERK) antibodies. (*B*) Livers were excised from *ob/ob* mice (six animals per group) treated with BSA (BSA), FGF19, or FGF19dCTD (at indicted doses) 5 h after injection. Tissue CYP7A1 mRNA levels were measured by quantitative RT-PCR.

with FGF19 (Fig. S3). As expected, however, βKlotho-stimulated interactions were abolished (Fig. 2*F*). These results suggest that the N-terminal region of FGF19 is sufficient to confer specific binding toward FGFR4. These data indicate that we have created an FGF19 molecule that can specifically activate only FGFR4-dependent signaling pathways.

Liver-Specific Activity of FGF19dCTD. Because there is a differential expression pattern of FGFRs in different tissues, we wanted to explore the ability of FGF19dCTD to activate signaling in target tissues, particularly fat and liver, in vivo. Various concentrations of FGF19 or FGF19dCTD were injected i.p. into *ob/ob* mice, tissues were collected 15 min after injection, and ERK phosphorylation was measured by Western blot analysis. Consistent with previous publications, FGF19 stimulated ERK phosphorylation in adipose tissue (Fig. 3*A*), but no ERK phosphorylation was observed in FGF19dCTD-treated mice (Fig. 3*A*). To further validate the lack of signaling in adipose, we tested FGF19dCTD in a glucose uptake assay using differentiated mouse 3T3-L1 adipocytes. As previously reported, FGF19 was able to stimulate glucose uptake in adipocytes, but this effect was not seen with FGF19dCTD treatment (Fig. 3*B*). Given that FGF19dCTD was unable to interact with βKlotho and induce βKlotho-dependent FGFR activation, these results suggest that βKlotho is essential for FGF19 to activate signaling in adipose tissue.

In contrast, ERK phosphorylation was observed in liver tissue as early as 15 min after injection in both FGF19- and FGF19dCTD-treated *ob/ob* animals (Fig. 4*A*). One major physiological function of FGF19 is the regulation of bile acid metabolism through the inhibition of CYP7A1 expression in the liver. We also found down-regulation of CYP7A1 expression in liver tissue from both FGF19- and FGF19dCTD-treated animals 5 h after injection (Fig. 4*B*). BSA injected at 10 mg/kg was used as a negative control to rule out any potential indirect effects on ERK phosphorylation because of injection of exogenous proteins. Based on our current in vitro data and the fact that FGFR4 is the major receptor in hepatocytes, we conclude that responsiveness to FGF19dCTD treatment in liver is mediated through FGFR4 activation in a βKlotho-independent manner. ERK
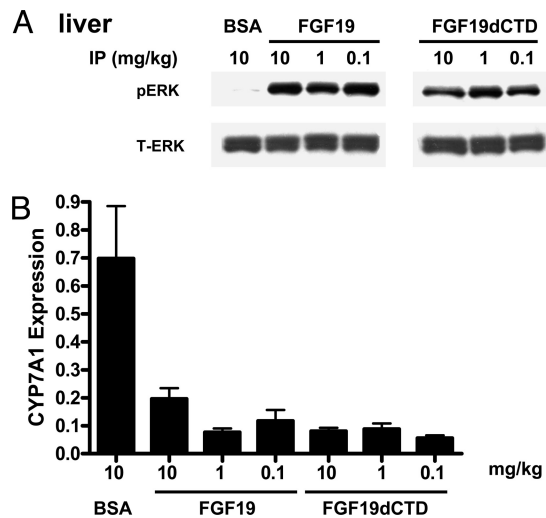
phosphorylation levels in several other tissues, such as skeletal muscle, have also been measured after treatment with FGF19 or FGF19dCTD. No significant changes were observed probably because of low FGFR4 expression levels (Fig. S4).

C-Terminal Tail Deletion Reduces the Glucose-Lowering Effect of FGF19. Because signaling by FGF19dCTD appeared to be FGFR4 selective, we wanted to explore the contribution of FGFR4 to the observed regulation of glucose homeostasis by FGF19. *Ob/ob* mice were sorted by body weight and plasma glucose levels and injected i.p. with a PBS control or indicated doses of FGF19 or FGF19dCTD (Fig. 5*A*). Blood glucose levels were measured at 0, 1, 3, and 5 h after injection, and the values are reported as area under the curve over this time period. Plasma glucose levels were significantly reduced in mice injected with FGF19 (10, 1, or 0.1 mg/kg) compared with the PBS control group ($P < 0.01$). However, acute glucose lowering was not observed in the group injected with FGF19dCTD (Fig. 5*A*) although the protein was found to activate liver signaling and inhibit CYP7A1 expression (Fig. 4).

The efficacy of various FGF molecules in the regulation of glucose metabolism was also examined in chronic studies. *Ob/ob* mice, sorted by body weight and plasma glucose levels, were injected daily with PBS, FGF19, or FGF19dCTD (5 or 1 mg/kg) for a period of 2 weeks. At the end of the treatment, fed plasma glucose levels were reduced by FGF19 treatment, but FGF19dCTD failed to reduce glucose levels. An oral glucose tolerance test was performed at the end of the 2-week treatment to assess the ability of the animals to dispose a glucose challenge. As shown in Fig. 5*B*, at both doses tested, FGF19 treatment significantly improved the response of animals to the oral glucose challenge. However, FGF19dCTD-treated mice failed to show improvement compared with the PBS control group (Fig. 5*B*). The lack of glucose effect by FGF19dCTD is not likely because of differential plasma stability of proteins, as both FGF19 and FGF19dCTD showed very similar pharmacokinetic properties in these animals (Fig. S5). These results suggest that although FGF19dCTD is able to activate FGFR4 signaling in the liver, it is insufficient to regulate and improve glucose homeostasis.
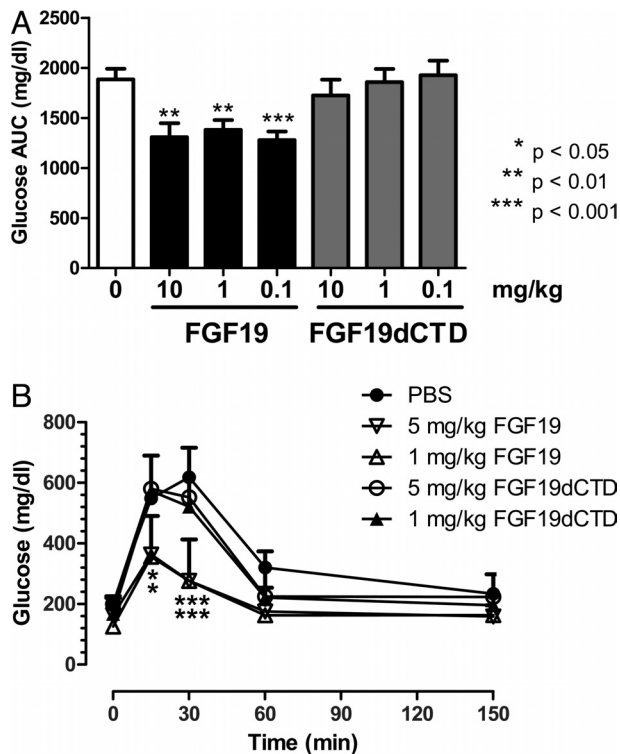
Fig. 5. Effects of FGF19 and FGF19dCTD on glucose metabolism. (*A*) *Ob/ob* mice were injected with recombinant FGF19 (*n* = 10) or FGF19dCTD (*n* = 10), plasma glucose levels were measured 1, 3, and 5 h after injection and plotted as area under the curve (AUC) during this time period. (*B*) *Ob/ob* mice were treated with FGF19 or FGF19dCTD for 12 days (once a day injection, 11 mice per group). An oral glucose tolerance test was performed after the glucose challenge.

Discussion

FGF19 is a unique member of the FGF family and is a novel hormone that regulates bile acid metabolism and glucose homeostasis. Although a co-receptor, βKlotho, was identified for FGF19 (11, 14, 17), potential differences in activation of different FGFRs by FGF19 and the contributions of other cofactors such as heparin are not well understood. By using co-transfection of various receptor combinations in L6 cells and with solid-phase binding studies, we observed differential interaction between FGF19 and the FGFRs. For FGFRs 1c, 2c, and 3c, βKlotho is an essential component for FGF19 interaction and activation of downstream signaling events. The weak heparin affinity does not contribute to either FGF19-FGFRs 1c, 2c, or 3c receptor interaction or receptor activation in the absence of βKlotho; therefore, FGF19 and FGF21 interact similarly with these receptors. However, in addition to βKlotho-induced FGF19 interaction and activation of FGFR4 (similar to FGFRs 1c, 2c, and 3c), FGF19 can also interact with and activate FGFR4 in the absence of βKlotho, promoted by its weak interaction with heparin. This is a notable feature for FGF19 that has not been observed for other subfamily members, FGF21 and FGF23.

Previous studies revealed that the C-terminal domain of FGF19 is necessary for βKlotho interaction and βKlotho-dependent receptor activation (12). Amino acid sequence alignments show that the C-terminal βKlotho binding domain is absent in other canonical FGFs, such as FGF1 and FGF2, suggesting that the FGF19 subfamily may have acquired this domain for Kotho-induced receptor interaction to compensate for dramatically weakened heparin-induced receptor interaction (5, 6, 11, 12). The only exception appears to be the FGF19/

FGFR4 interaction, where FGF19 has retained its ability to interact with and activate FGFR4 in the absence of βKlotho, mediated by its weak interaction with heparin. We previously showed that the N-terminal region of FGF19 is responsible for heparin-dependent FGFR interactions (12). Given that FGF19 can activate FGFR4 in the absence of βKlotho, we hypothesized that the N-terminal region of FGF19 may be sufficient for FGFR4 activation, but would be inactive with other receptors that require the βKlotho co-receptor for FGF19-dependent signaling. Therefore, we generated and purified a truncated FGF19 molecule, FGF19dCTD, by removing the C-terminal 40 amino acid residues and we characterized its activity biochemically, on cells and in animals. Consistent with our hypothesis, FGF19dCTD activated FGFR4 but lost the ability to activate other FGF receptors, even in the presence of βKlotho. FGF19dCTD appears to be an FGFR4-specific activator.

In animals injected with FGF19dCTD, ERK phosphorylation was observed in liver (where FGFR4 is predominantly expressed) but not in adipose tissue (where FGFR1c and 2c are the predominant receptors). Consistent with the signaling specificity observed in vitro, FGF19dCTD suppressed the expression of the CYP7A1 target gene in liver, presumably mediated through FGFR4 activation in a βKlotho-independent manner. Studies with βKlotho knockout mice indicate that it is involved in the regulation of CYP7A1 expression (18). We observed that βKlotho significantly increased FGF19 potency on FGFR4 activation in vitro (Fig. 1*D*). We speculate that because the normal concentration of FGF19/FGF15 in plasma is low, βKlotho is critical in conferring FGFR4 activation under physiological conditions. Our experiments were performed with supraphysiological levels of recombinant proteins. Although this might not occur under physiological conditions, FGFR4 activation achieved under high FGF19 concentrations independent of βKlotho may result in functional end points similar to activation via βKlotho-dependent conditions.

The ability of FGF19dCTD to inhibit liver CYP7A1 mRNA expression suggests that this FGFR4-specific activator may still be able to regulate bile acid metabolism similar to wild-type FGF19. However, the ability of regulating glucose metabolism was lost with this truncated FGFR4-specific activator (Fig. 5). This would suggest that the regulation of liver bile acid metabolism by FGF19 could be independent of its effects on glucose homeostasis, and FGF19dCTD could serve as a useful tool for studying these two functions separately. These findings may also suggest that activation of target tissues other than liver, including adipose, may provide significant contributions in the regulation of glucose homeostasis. The inability of FGF19dCTD to regulate glucose metabolism is somewhat surprising given that FGFR4 knockout mice display glucose intolerance and insulin-resistant phenotypes (19), and that FGF19 has been shown to induce phosphorylation of FoxO1, a key regulator of glucose metabolism, in primary mouse hepatocytes through FGFR4 (20). Additional studies will be required to further address the contribution of liver FGFR signaling to glucose regulation by FGF19 and other subfamily members, such as FGF21.

In summary, our studies suggest that improvement of glucose homeostasis after treatment with recombinant FGF19 is likely because of the direct activation of FGF receptor signaling in adipose and other target tissues and not through liver FGFR4 activation.

Materials and Methods

Expression and Purification of Recombinant FGF19 and FGF19DCTD. DNA encoding wild-type FGF19 or FGF19DCTD (residues 1–156) were cloned into the pET30 vector (Novagen). DNA constructs were transformed into BL21(DE3) *E. coli* (Novagen). Protein expression was induced with IPTG at 37 °C. Purification was as previously described (12).

Cell Culture and Transfections. L6 cells were maintained in DMEM supplemented with 10% FBS (FBS) and penicillin/streptomycin. Cells were transfected with expression vectors using the Lipofectamine 2000 transfection reagent (Invitrogen) according to the manufacturer's protocol.

Western Blot Analysis of FGF Signaling. Analysis of FGF signaling in L6 cells was performed as previously described (12). Liver and adipose tissues were collected 15 min after injection and snap frozen in liquid nitrogen, homogenized in lysis buffer, and subjected to western blot analysis using an anti-phospho-p44/42 MAP kinase (ERK1/2) antibody and an anti-ERK antibody (Cell Signaling).

MSD Assay. L6 cells plated in 24-well plates (10^6 cells/well) were transfected with expression vectors for various FGF receptors and αKlotho/βKlotho and serum starved in 0.2% BSA overnight before treatments. Media was aspirated 10 min after treatment and plates were snap frozen in liquid nitrogen. Cells in each well were lysed in 60 μL complete lysis buffer and total and phosphorylated ERK were measured using an MSD whole cell lysate Phospho-ERK1/2 kit (Meso Scale Discovery) according to the manufacturer's instructions.

Solid-Phase Binding Assay. Nunc Maxisorp 96-well plates were coated overnight at 4 °C degrees with 50 μL of 2 μg/mL AffiniPure Rabbit Anti-Human IgG, Fcγ Fragment Specific Antibody (Jackson ImmunoResearch). Plates were washed four times with PBS containing 0.05% Tween-20 and then blocked with PBS containing 3% BSA for 2 h at room temperature. Following another wash, 100 μL of 1 μg/mL FGFR1c-Fc or FGFR4-Fc was added and plates were incubated for 1 h at room temperature. Plates were washed again and 45 μL of 0.5 μg/mL His-tagged soluble recombinant βKlotho protein or vehicle was added to each well. After 1.5 h, biotinylated FGF proteins (FGF proteins were biotinylated with Pierce Sulfo-NHS-LC-Biotin), in the presence or absence of 10 μg/mL heparin (Sigma), were added and the plates incubated for another 1.5 h at room temperature. The plates were then washed and streptavidin-HRP (R&D Systems) was used for detection.

Animals and Treatments. Age-matched C57BL/6 or *ob/ob* mice were used in the studies. Purified FGF19, FGF19dCTD, or vehicle (PBS) was injected i.p. at stated concentrations. After indicated times, tail vein blood was collected and blood glucose was measured by a glucose meter (BD). For chronic treatment, mice were injected once daily for 12 days before tissue collection.

Oral Glucose Tolerance Test. After overnight fasting, mice were injected with a bolus of glucose (1 g/ kg body weight) into the stomach by a gavage needle (20 Ga × 1–1/2′′, Popper and Sons Inc.) and 30 μL blood was sampled at 0, 15, 30, 60, and 120 min for plasma glucose analysis. Plasma glucose was measured by using Glucose Assay Reagent (Sigma).

Glucose Uptake Assay. 3T3L1 preadipocytes (ATCC CL-173) were cultured and induced to differentiate as follows: Cells were plated in Dulbecco's Modified Eagle's Medium (DMEM) with 10% fetal FBS and 1% Pen-Strep at a density of 25,000 cells per well on 96-well Cytostar-T scintillating microplates (GE Healthcare). Two days after reaching confluence, differentiation was induced by adding 250 nM dexamethasone (Sigma), 500 μM isobutylmethylxanthine (Sigma) and 1 μg/mL insulin (Sigma) into basic culture medium for 2 days. The cells were then cultured in DMEM with 10% FBS, 1% Pen-Strep and 1 μg/mL insulin for 2 days, and basic culture medium for an additional 3 days. Seven days after induction, differentiated adipocytes were washed once with DMEM containing 1% FBS and 1% Pen-Strep. Treatments were added to the adipocytes at the indicated concentrations in DMEM with 1% FBS and 1% Pen-Strep, and the adipocytes were incubated for 72 h. The cells were then washed once with glucose-free DMEM (Invitrogen) containing 0.1% fatty-acid free BSA, and treatments were added to the cells at the indicated concentrations in the same medium. After 2.5 h of incubation, insulin was added at the indicated concentrations to wells containing glucose-free DMEM and 0.1% fatty-acid free BSA, and the cells were incubated for an additional 30 min. The cells were then washed twice with Krebs-Ringer Phosphate Buffer (KRP) composed of 118 mM NaCl, 4.8 mM KCl, 1.3 mM CaCl$_2$, 1.2 mM KH$_2$PO$_4$, 1.2 mM MgSO$_4$, and 15 mM HEPES (pH 7.4), with 0.1% fatty-acid free BSA added. Cells were treated with FGF19 at the indicated concentrations in KRP containing 0.1% fatty-acid free BSA. 2-Deoxyglucose-1-^{3}H (Sigma) was added to the cells at a concentration of 0.2 μCi per well and they were incubated for 1 h at 37 °C. Cytochalasin B (50 μM) (Sigma) was added to the cells to terminate the reaction and deoxyglucose uptake was measured on a Wallac MicroBeta (Perkin-Elmer). Nonspecific deoxyglucose uptake was measured in the presence of 50 μM cytochalasin B and subtracted from each sample to obtain specific uptake.

Quantitative RT-PCR. Total RNA was isolated using the QIAcube and the RNeasy kit (Qiagen) with DNase treatment. Quantitative RT-PCR reactions contained 100 ng of isolated total RNA, 200 nM of each gene specific primer and probe, and Brilliant II QRT-PCR Master mix (Stratagene), in a total volume of 50 μL. All of the reactions were performed in duplicate on a Stratagene MX3000p sequence detection system, and relative mRNA levels were calculated by the comparative threshold cycle method using GAPDH as the internal control.

1. Inagaki T, et al. (2005) Fibroblast growth factor 15 functions as an enterohepatic signal to regulate bile acid homeostasis. *Cell Metab* 2:217–225.
2. Fu L, et al. (2004) Fibroblast growth factor 19 increases metabolic rate and reverses dietary and leptin-deficient diabetes. *Endocrinology* 145:2594–2603.
3. Coskun T, et al. (2008) FGF21 corrects obesity in mice. *Endocrinology* 149:6018–6027.
4. Yu X, White KE (2005) FGF23 and disorders of phosphate homeostasis. *Cytokine Growth Factor Rev* 16:221–232.
5. Goetz R, et al. (2007) Molecular insights into the klotho-dependent, endocrine mode of action of fibroblast growth factor 19 subfamily members. *Mol Cell Biol* 27:3417–3428.
6. Asada M, et al. (2008) Glycosaminoglycan affinity of the complete fibroblast growth factor family. *Biochim Biophys Acta* 1790:40–48.
7. Harmer NJ, Pellegrini L, Chirgadze D, Fernandez-Recio J, Blundell TL (2004) The crystal structure of fibroblast growth factor (FGF) 19 reveals novel features of the FGF family and offers a structural basis for its unusual receptor affinity. *Biochemistry* 43:629–640.
8. Ogawa Y, et al. (2007) BetaKlotho is required for metabolic activity of fibroblast growth factor 21. *Proc Natl Acad Sci USA* 104:7432–7437.
9. Urakawa I, et al. (2006) Klotho converts canonical FGF receptor into a specific receptor for FGF23. *Nature* 444:770–774.
10. Kuro-o M (2006) Klotho as a regulator of fibroblast growth factor signaling and phosphate/calcium metabolism. *Curr Opin Nephrol Hypertens* 15:437–441.
11. Wu X, et al. (2007) Co-receptor requirements for fibroblast growth factor-19 signaling. *J Biol Chem* 282:29069–29072.
12. Wu X, et al. (2008) C-terminal tail of FGF19 determines its specificity toward klotho co-receptors. *J Biol Chem* 283:33304–33309.
13. Xie MH, et al. (1999) FGF-19, a novel fibroblast growth factor with unique specificity for FGFR4. *Cytokine* 11:729–735.
14. Kurosu H, et al. (2007) Tissue-specific expression of betaKlotho and fibroblast growth factor (FGF) receptor isoforms determines metabolic activity of FGF19 and FGF21. *J Biol Chem* 282:26687–26695.
15. Holt JA, et al. (2003) Definition of a novel growth factor-dependent signal cascade for the suppression of bile acid biosynthesis. *Genes Dev* 17:1581–1591.
16. Tomlinson E, et al. (2002) Transgenic mice expressing human fibroblast growth factor-19 display increased metabolic rate and decreased adiposity. *Endocrinology* 143:1741–1747.
17. Lin BC, Wang M, Blackmore C, Desnoyers LR (2007) Liver-specific activities of FGF19 require Klotho beta. *J Biol Chem* 282:27277–27284.
18. Ito S, Fujimori T, Furuya A, Satoh J, Nabeshima Y, Nabeshima Y (2005) Impaired negative feedback suppression of bile acid synthesis in mice lacking betaKlotho. *J Clin Invest* 115:2202–2208.
19. Huang X, Yang C, Luo Y, Jin C, Wang F, McKeehan WL (2007) FGFR4 prevents hyperlipidemia and insulin resistance but underlies high-fat diet induced fatty liver. *Diabetes* 56:2501–2510.
20. Shin DJ, Osborne TF (2009) FGF15/FGFR4 integrates growth factor signaling with hepatic bile acid metabolism and insulin action. *J Biol Chem* 284:11110–11120.